NANO LETTERS

Letter

pubs.acs.org/NanoLett

van der Waals Force: A Dominant Factor for Reactivity of Graphene

Jong Hak Lee,*[,†,‡,∇] Ahmet Avsar,[†,‡,∇] Jeil Jung,[†,‡] Jun You Tan,[‡] K. Watanabe,[⊥] T. Taniguchi,[⊥] Srinivasan Natarajan,[†,‡] Goki Eda,[†,‡,#] Shaffique Adam,[†,‡,∥] Antonio H. Castro Neto,[†,‡] and Barbaros Özyilmaz*[,†,‡,§]

[†]Department of Physics, National University of Singapore, Singapore 117542, Singapore

[‡]Centre for Advanced 2D Materials and Graphene Research Center, National University of Singapore, Singapore 117542, Singapore

[§]NanoCore, National University of Singapore, Singapore 117576, Singapore

[∥]Yale-NUS College, 6 College Avenue East, Singapore 138614, Singapore

[⊥]Advanced Material Laboratory, National Institute for Materials Science, 1-1 Namiki, Tsukuba 305-0044, Japan

[#]Chemistry Department, National University of Singapore, 3 Science Drive 3, Singapore 117543, Singapore

Supporting Information

ABSTRACT: Reactivity control of graphene is an important issue because chemical functionalization can modulate graphene's unique mechanical, optical, and electronic properties. Using systematic optical studies, we demonstrate that van der Waals interaction is the dominant factor for the chemical reactivity of graphene on two-dimensional (2D) heterostructures. A significant enhancement in the chemical stability of graphene is achieved by replacing the common SiO_2 substrate with 2D crystals such as an additional graphene layer, WS_2, MoS_2, or h-BN. Our theoretical and experimental results show that its origin is a strong van der Waals interaction between the graphene layer and the 2D substrate. This results in a high resistive force on graphene toward geometric lattice deformation. We also demonstrate that the chemical reactivity of graphene can be controlled by the relative lattice orientation with respect to the substrates and thus can be used for a wide range of applications including hydrogen storage.

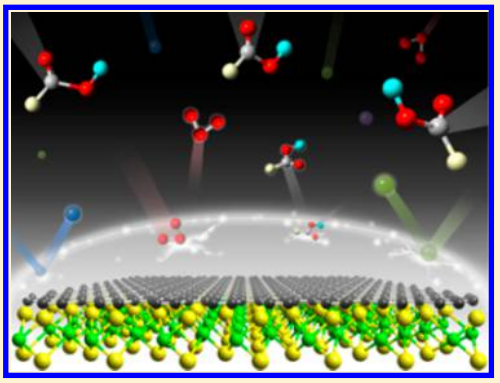

KEYWORDS: *van der Waals interaction, 2D heterostructures, chemical reactivity, graphene, hydrogen storage, functionalization*

Recently, research interest in atomically thin two-dimensional (2D) materials has expanded to include van der Waals (vdW) 2D heterostructures, which can be fabricated by stacking different 2D crystals.[1−3] Strong covalent bonds provide in-plane stability to the 2D crystals, whereas the relatively weak vdW force is sufficient to keep the stack together.[3] The layer by layer assembly has shown unusual and extraordinary properties such as 10-fold increase in electronic quality of graphene on hexagonal boron nitride (h-BN) substrate.[1] Additionally, vdW heterostructures have also attracted immediate attention for flexible and transparent electronics applications. However, most studies have narrowly focused on the electrical properties and device applications, whereas other properties have been left unexplored.[1−3]

In this work, we investigate the chemical reactivity of two-dimensional (2D) heterostructures through systematic optical studies. We used graphene as a top layer of the vdW heterostructures because graphene's optical properties are relatively well studied among 2D crystals. In addition, graphene has been considered as a very promising material for flexible and transparent electronics applications because of its extraordinary electronic and mechanical properties resulting from a perfect hexagonal crystal lattice.[4−6] However, graphene has a molecule-like sensitivity to its surroundings because every atom in graphene is exposed to the surface.[7] The interaction of a pristine graphene lattice with a disordered environment can alter the former's properties.[8,9] Therefore, it is important to develop strategies to protect graphene from interactions with its environment. Here, we demonstrate a significant enhancement in chemical stability of graphene supported on a wide range of vdW interactive substrates such as a second graphene layer, WS_2, MoS_2, or h-BN. On the basis of our experimental and theoretical analysis, we found that the strength of the vdW coupling and local stacking coordination between graphene and the substrate are the dominant factors responsible for the chemical reactivity of graphene.

In order to investigate the degree of chemical stability of graphene heterostructures in a reactive atmosphere, we carried out ultraviolet (UV)/ozone treatment on different types of graphene samples, such as single layered graphene on a SiO_2 coated wafer (SLG/SiO_2), Bernal stacked bilayer graphene on a SiO_2 coated wafer (BLG/SiO_2), twisted bilayer graphene on a

Received: September 18, 2014
Revised: November 11, 2014

   dx.doi.org/10.1021/nl5036012 | *Nano Lett.* XXXX, XXX, XXX−XXX

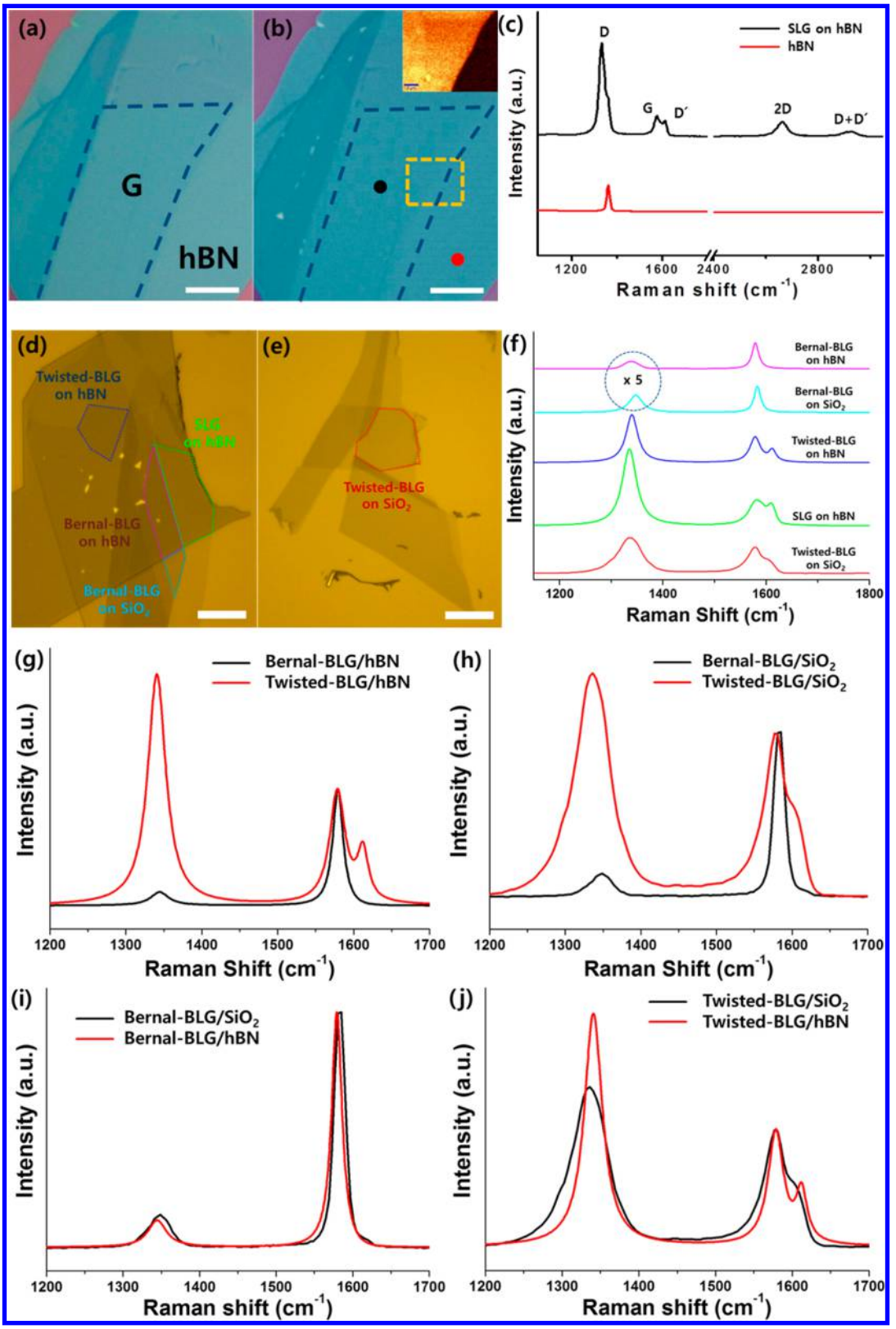

Figure 1. Optical and Raman studies with and without UV/ozone treatment. Optical images of SLG on hBN flake before (a) and after treatment (b), respectively. (c) Raman spectrum results of each part of panel b. Inset of panel b shows the Raman mapping image of G band of the region inside the dashed rectangle. (d,e) Optical images of vdW heterostructures and (f) Raman spectrum results of each part after UV/ozone treatment. (g,h) Stacking order effect on bilayered graphene on hBN. (i,j) Roughness and charge inhomogeneity effect on bilayered graphene. All scale bars are 10 μm.

SiO_2 coated wafer (twisted-BLG/SiO_2), single layered graphene on a hexagonal boron nitride flake (SLG/hBN), Bernal stacked bilayer graphene on a hexagonal boron nitride flake (BLG/hBN), and twisted bilayer graphene on a hexagonal boron

dx.doi.org/10.1021/nl5036012 | *Nano Lett.* XXXX, XXX, XXX−XXX

nitride flake (twisted-BLG/hBN). The treatments were done using an UV/ozone cleaner (UV/Ozone procleaner, BioForce). UV/ozone induced etching of graphene has been studied since UV/ozone is a severely corrosive environment for graphene.[10,11] In our experiments, the SLG/SiO_2 was completely removed after 5 min of treatment as shown in Figure S1, Supporting Information. However, all graphene heterostructures survived the same severe condition. Figure 1a,b shows that the optical images of SLG on hBN flake before and after treatment, respectively. The inset of Figure 1b clearly shows that graphene still exists on h-BN. From Raman spectrum result (Figure 1c), the defect density (n_D) of the SLG/hBN can be estimated using the relation $L_D^2(\mathrm{nm}^2) = (1.8 \pm 0.5) \times 10^{-9}\lambda_L^4(I_G/I_D)$ and $n_D(\mathrm{cm}^{-2}) = 10^{14}/(\pi L_D^2)$; where L_D is separation between defects, λ_L is the wavelength of the exciting laser of Raman spectrum = 532 nm, I_G is intensity of G peak, and I_D is intensity of D peak.[12−14] The obtained L_D and n_D are 1.2 nm and $2.2 \times 10^{13}/\mathrm{cm}^2$, respectively. Thus, the SLG/hBN has only 0.58% defective area, while the SLG/SiO_2 is completely etched away. Figure 1d,e shows the optical images of BLG/SiO_2, twisted-BLG/SiO_2, SLG/hBN, BLG/hBN, and twisted-BLG/hBN before and after treatment, respectively. From the graphene heterostructures' Raman spectrum results (Figure 1f−j), we found that the stacking order of bilayer graphene strongly affects its chemical reactivity. The Bernal stacked bilayer graphene parts (BLG/SiO_2 and BLG/hBN) have very small amount of disorder compared to the twisted bilayer graphene region (twisted-BLG/SiO_2 and twisted-BLG/hBN) as shown in Figure 1g−j. Most notably, BLG/SiO_2 has higher chemical stability than SLG/hBN and twisted-BLG/hBN.

To eliminate the possibility of gas intercalation between graphene and substrate through the edge of the graphene layer and confirm that functionalization happens only on the basal plane, we introduced hydrogenation to graphene using electron beam (e-beam) lithography on hydrogen silsesquioxane (HSQ) resist, as we have reported previously.[8] We transferred single layer graphene onto molybdenum disulfide (SLG/MoS_2) and tungsten disulfide (SLG/WS_2). In this experiment, samples were annealed at 340 °C for 6 h in Ar/H_2 (9/1) gaseous mixture to remove possible tape and transfer resist residues. For comparison, we also prepared single layered graphene and Bernal stacked bilayer graphene on SiO_2 coated wafer (SLG/SiO_2 and BLG/SiO_2). After spin coating HSQ on the samples, we irradiated e-beam (dose of 2−8 $\mathrm{mC/cm}^2$) onto each sample. We confirmed that hydrogenation happens only on the e-beam exposed areas (see Supporting Information) and the intensity of the D band is proportional to the hydrogen coverage.[8,9] After e-beam irradiation, the degree of structural deformation of graphene was characterized by Raman spectroscopy. The Raman spectra results clearly show the difference in D band intensities. As shown in Figure 2, the SLG/SiO_2 has higher D band intensity with increasing e-beam dose. However, BLG/SiO_2 has a small D peak (D/G ratio is about 0.1) upon an e-beam dose of 8 $\mathrm{mC/cm}^2$. Surprisingly, SLG/MoS_2 and SLG/WS_2 do not have any D band even after 8 $\mathrm{mC/cm}^2$ of e-beam irradiation. This strongly suggests that the chemical stabilities of SLG/MoS_2 and SLG/WS_2 are much higher than those of SLG/SiO_2 and BLG/SiO_2.

It is widely believed that only local curvature[15,16] and charge density inhomogeneity[17,18] are responsible for the chemical reactivity of graphene. However, our experimental data cannot be understood within either of these frameworks. For example,

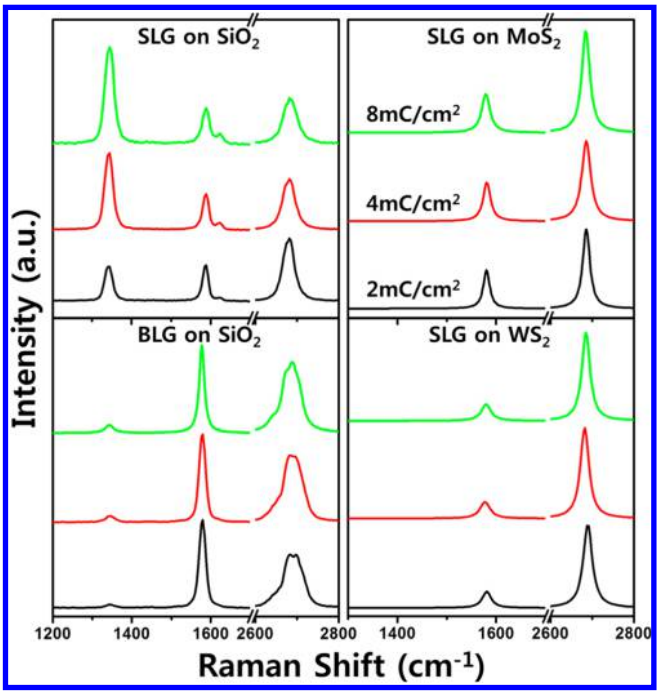

Figure 2. Raman study of hydrogenated graphene heterostructures. Raman spectra of SLG/SiO_2, BLG/SiO_2, SLG/MoS_2, and SLG/WS_2 after HSQ treatments with various e-beam doses (black, 2 $\mathrm{mC/cm}^2$; red, 4 $\mathrm{mC/cm}^2$; green, 8 $\mathrm{mC/cm}^2$).

we find that the BLG/SiO_2 has a much larger surface roughness than monolayer graphene on h-BN (see Figure S2, Supporting Information), yet we find that the monolayer is far more reactive. Similarly, the charge density inhomogeneity of bilayer graphene is much larger than that of monolayer graphene,[19] and so the notion that charge density fluctuations are responsible for the reactivity of our samples is inconsistent with our observations. As we discuss below, we find that the interlayer binding energy of graphene with its 2D crystal substrate has the largest influence on the chemical reactivity of graphene. When two different atomic layers are near each other, the binding configuration can be determined by direct covalent or ionic bonds depending on the materials' nature as well as vdW interactions. Those covalent or ionic bonds can affect the chemical reactivity very much. Two-dimensional (layered structure) crystals have strong covalent bonds in-plane, whereas the relatively weak vdW force out-of-plane is sufficient to keep the stack together[3] even in a van der Waals heterostructure. We have confirmed that there is no functionalization using Raman spectroscopy. We have also confirmed that graphene keeps its unique electrical property on other 2D crystals through resistivity measurements as a function of V_{BG} at room temperature (Figure S5, Supporting Information). A graphene layer naturally has vdW mediated bonds with its neighboring layers in graphite.[4] Single layer h-BN, WS_2, and MoS_2 have an atomically thin, smooth surface, which results in the vdW interaction with graphene.[3] In the atomic scale, therefore, atoms in the top graphene layer and the underlying layer (second graphene layer or 2D crystals) are at an equilibrium distance, i.e., at the minimum of its total energy curve (Figure 3e). In addition, in the honeycomb lattice of graphene, each carbon atom has a 3-fold symmetric sp^2 hybridization.[4] Disrupting this structure is not only thermodynamically unfavorable but requires also the formation of high energy

dx.doi.org/10.1021/nl5036012 | Nano Lett. XXXX, XXX, XXX−XXX

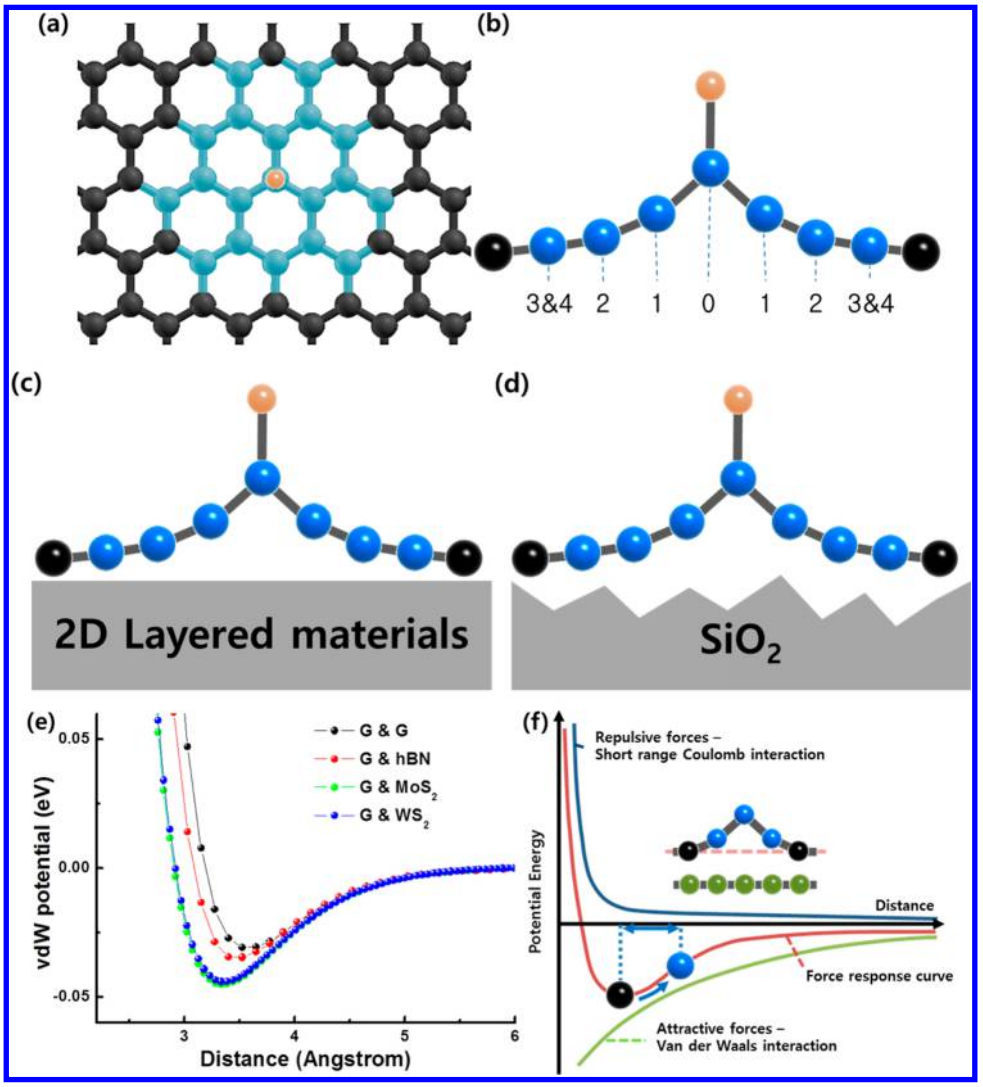

Figure 3. (a–d) Local distortions around functionalized C atom due to H chemisorption and situations of hydrogenated graphene with 2D layered materials and SiO_2. (e) vdW potential energy curves plotted as a function of the vdW gap for various heterostructures. (f) Atomic configuration of the functionalized graphene and 2D substrate and its energy diagram.

radicals localized on adjacent carbon atoms.[20,21] Covalent functionalization on the basal plane of graphene is further hindered by a high kinetic barrier associated with tetrahedral geometric rearrangements of the carbon lattice.[20,21] In other words, this transformation affects not only sp^3 carbons directly functionalized by the reaction but creates also a geometric distortion that extends over multiple lattice positions. As shown in Figure 3a,b, when a reactive ion such as hydrogen or oxygen ion attaches to the graphene lattice, the functionalized atom moves along the out-of-plane direction, and because of that, the neighboring atoms rearrange by moving in both in-plane (lateral shift, Figure 3a) and out-of-plane (upward, Figure 3b) directions. Through the simulation based on local density approximation (LDA), we found that the puckering height of the hydrogen bonded carbon atom reaches about 0.48 Å. From the first neighboring atoms to fourth neighboring atoms, the in-plane and out-of-plane displacements gradually decrease. On the basis of the simulation results, we infer that in order to functionalize the top graphene layer, which has vdW interactions with the substrate, reactive ions need additional energy for functionalization compared to free-standing graphene. In other words, graphene on a vdW interactive substrate exerts a resistive force toward the reactive environments. In order to investigate the influence of vdW interlayer coupling on hydrogenation of graphene, we have performed self-consistent LDA calculations of a hydrogen atom adsorbed on single-layer graphene and bilayer graphene. Even though the LDA does not capture the many-body effects in the nonlocal dispersive vdW interactions, its tendency to overbind covalent bonds allows holding together the weakly interacting layers. This results in geometries and forces that are in reasonable agreement with more sophisticated calculations like random phase approximation (RPA) total energy based calculations in thin jellium metal slabs,[22] hexagonal boron nitride,[23] or graphite[24] and other layered 2D materials.[25] We compared total energy differences between pristine and chemisorbed conditions.

The Figure 4a,c shows the buckled geometry of graphene in the presence of a chemisorbed H atom. A similar geometry correction takes place in bilayer graphene as shown in Figure 4b,d, but with suppressions in the relative distances between the neighboring carbon atoms compared to single layer graphene (Table 1). The total binding energy of H on graphene ($E_b = E_G + E_H - E_{G+H}$) is approximately 2.9 eV for

dx.doi.org/10.1021/nl5036012 | Nano Lett. XXXX, XXX, XXX–XXX

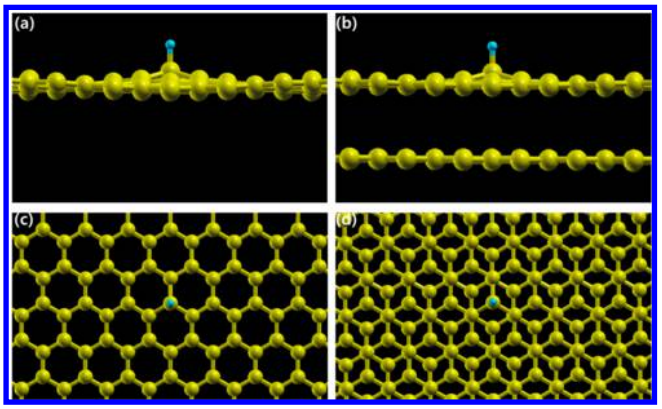

Figure 4. (a,c) Top and side views of a functionalized graphene sheet. (b,d) Top and side views of a functionalized bilayered graphene sheet with a chemisorbed H atom. We can clearly observe the buckling of the carbon atoms that acquire partial sp^3 hybridization.

Table 1. Differences between the Neighboring Position of the Carbon Atoms $d_m - d_{m+1}$ in Å, Their in-Plane Distance Differences $xy_m - xy_{m+1}$ with Respect to the Equilibirum, and Differences in Vertical Shifts $z_m - z_{m+1}$, Starting from m = 0, the Chemisorbed Carbon Site, until the Third Nearest Neighbor as Illustrated in Figure 4

	graphene			bilayered graphene		
m	0	1	2	0	1	2
$d_m - d_{m+1}$	0.068	−0.032	−0.012	0.055	−0.0309	−0.006
$xy_m - xy_{m+1}$	0.035	0.034	−0.012	0.021	−0.0317	−0.006
$z_m - z_{m+1}$	0.309	0.069	−0.020	0.317	0.048	−0.018

chemisorption on single layer graphene and 0.9 eV for that on bilayer graphene. We note that the generalized gradient approximation (GGA) is expected to be quantitatively more accurate in obtaining chemisorption energies, but the LDA calculation was used here because it is able to bind the layers within the same self-consistent calculation framework. The above energy differences clearly indicate that the chemisorption of an H atom on single layer graphene is approximately three times more favorable, from the total energy perspective, than the chemisorption on bilayer graphene. The only difference between these two systems is the presence of an additional supporting graphene layer in the bilayer graphene structure. The origin of this behavior has to be attributed to the interlayer interaction between graphene sheets, which prevents the buckling and in-plane strains of the top graphene sheet when the hydrogen atom is deposited. In other words, the vdW force, which is well-known as the weakest force between atoms or molecules, strongly affects the chemical reactivity of the top graphene layer. We also conclude that the vdW interaction effect on graphene's chemical stability is a much more dominant factor than local curvature effects and charge density inhomogeneity effects when they coexist. This becomes clear when one compares Raman spectra as shown in Figure 1g–j.

The vdW-interaction-incorporated graphene hydrogenation simulation results clearly support the enhanced chemical stability of 2D heterostructures, whereas the degree of chemical stability of graphene heterostructures can be explained by the quality of the interfaces. The BLG/SiO_2 was prepared by mechanical exfoliation from highly crystalline natural graphite, and BLG naturally has Bernal stacking between graphene layers. However, twisted-BLG/SiO_2, SLG/hBN, and twisted-BLG/hBN heterostructures were fabricated by an additional transfer method after mechanical exfoliation. Therefore, the interfaces of those heterostructures are expected to have a poorer vdW interaction due to the lattice mismatch and larger equilibrium distances than that of Bernal stacked bilayer graphene, thus resulting in weaker chemical stabilities of twisted-BLG/SiO_2, SLG/hBN, and twisted-BLG/hBN than that of BLG/SiO_2. In addition, we can infer that graphene–dichalcogenide heterostructures should be more stable than other heterostructures because of the stronger vdW binding energies between graphene and 2D substrates, obtained from the vdW interaction energy curves. In order to compare the chemical reactivities of BLG/SiO_2 and graphene–dichalcogenide heterostructures in a severely reactive condition, we treated BLG/SiO_2 and SLG/MoS_2 with O_2 plasma. Figure 5a,b shows the optical images of Bernal stacked bilayered graphene and SLG on MoS_2 heterostructures. Figure 5c clearly shows that the disordered structure peak (D peak) of BLG/SiO_2 is broader and stronger than that of SLG/MoS_2 after O_2 plasma treatment.

Our findings have strong implications in design strategies of graphene/graphite electrodes for hydrogen storage.[26,27] Graphene has been investigated as a promising material for hydrogen storage because the maximum achievable gravimetric density of hydrogen in graphene with chemisorption is 8.3%.[26,27] The chemisorbed hydrogen, however, can only be released at high temperatures (>650 K), thus the problem of desorption of molecular hydrogen remains the bottleneck for considering such a system for practical purposes. Thus, any

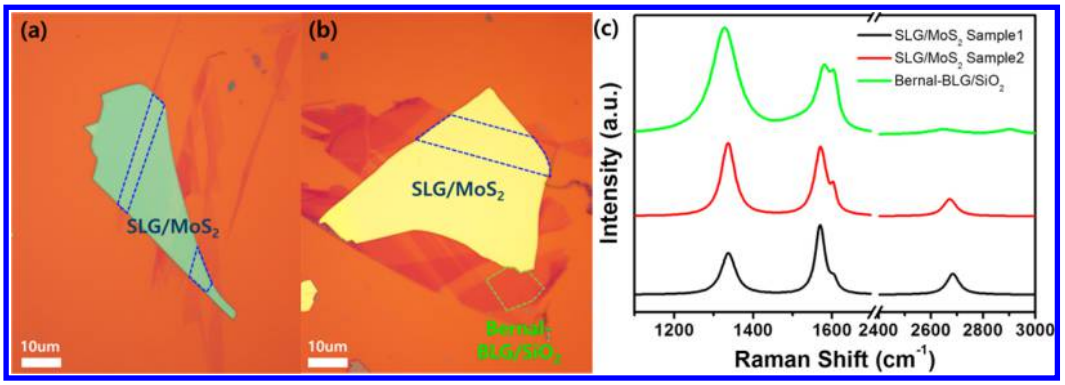

Figure 5. Optical images and Raman studies of Bernal stacked bilayered graphene and SLG on MoS_2 heterostructures with O_2 plasma treatment. SLG/MoS_2 structures have lower and narrower D band compared to the Bernal-BLG/SiO_2 structure.

dx.doi.org/10.1021/nl5036012 | Nano Lett. XXXX, XXX, XXX–XXX

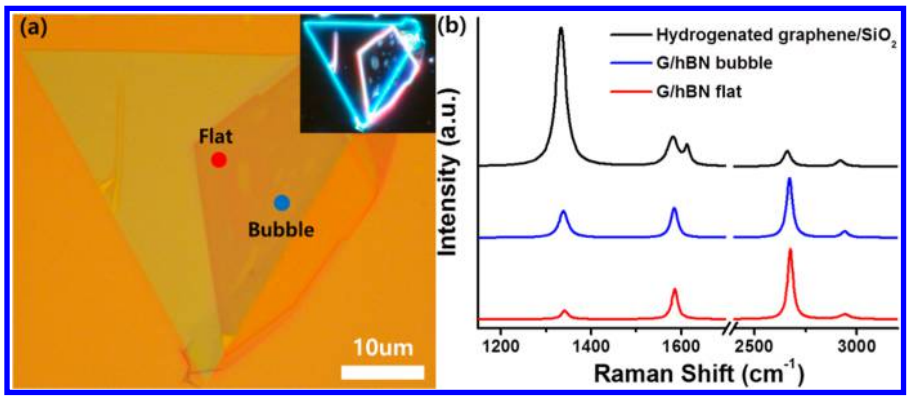

Figure 6. (a) Optical image of single layered graphene on hBN after transfer step. Inset shows dark field images of vdW heterostructure of hydrogenated graphene on h-BN. (b) Raman spectrum results of hydrogenated SLG before transfer and flat and bubble regions after transfer.

efficient hydrogen storage device must consider ways to overcome such energy barriers.[26,27] In order to solve the dehydrogenation barrier problem, we have investigated whether vdW interactive substrates can help release hydrogen atoms from hydrogenated graphene. We hydrogenated graphene on SiO_2 with HSQ treatment for efficient functionalization. As shown in Figure 6a,b, as-prepared hydrogenated graphene has a high D band in its Raman spectrum. After functionalization, we transferred the hydrogenated graphene on to an h-BN substrate. Surprisingly, the hydrogenated graphene was dehydrogenated by a simple physical transfer without any annealing. The Raman D band decreased drastically in intensity relative to the G band. The I_D/I_G ratio decreases by a factor of more than 16, from 4.9 to 0.3. Through the dark field image we can easily observe the bubbles and the flat region obviously. The bubble region is where the graphene does not have a proper van der Waals interaction with the substrate, so compared to the flat region the degree of reduction of hydrogen is lower in this bubble region. This experiment successfully demonstrated that vdW interactive substrates can help decrease the energy barrier and release hydrogen atoms from hydrogenated graphene.

In summary, we found that the physical lattice orientation of graphene and substrates and their van der Waals interactions can govern chemical reaction at the atomic scale in striking contrast to conventional chemical reactivity theory of solid surfaces. The latter is generally defined by the chemical potential of the surface atoms and is independent of the bulk properties. We demonstrated a high chemical stability enhancement of graphene with vdW interactive 2D crystal structures such as a second graphene layer, WS_2, MoS_2, and h-BN. Theoretical and experimental results demonstrated that the vdW layer coupling is the main driving factor in reactivity suppression by providing a higher resistive force toward geometric lattice deformation. This study provides a practical protection strategy for 2D materials without "physical screening" from the reactive side by employing vdW interactive substrates and also an effective solution for hydrogen storage.

■ ASSOCIATED CONTENT

Ⓢ Supporting Information

Experimental, additional AFM and photo images, and functionalization of graphene data. This material is available free of charge via the Internet at http://pubs.acs.org.

■ AUTHOR INFORMATION

Corresponding Authors

*E-mail: ljhacy@gmail.com.
*E-mail: phyob@nus.edu.sg.

Author Contributions

$^{\nabla}$These authors contributed equally to this work.

Notes

The authors declare no competing financial interest.

■ ACKNOWLEDGMENTS

We thank Dr. Simone Casolo for discussions. This research is supported by the National Research Foundation, Prime Minister's Office, Singapore, under its Competitive Research Programme (CRP Award No. NRF-CRP9-2011-3 and NRF-CRP6-2010-5), Research Fellowship (RF Award No. 224 NRF-RF2008-7, NRF-NRFF2011-02, and NRF-NRFF2012-01), NUS Young Investigator Award, and SMF-NUS Research Horizons Award 2009-Phase II. We acknowledge use of computational resources from the Texas Advanced Computing Center and the high performance computing center at the Graphene Research Centre at the National University of Singapore

■ REFERENCES

(1) Dean, C. R.; Young, A. F.; Meric, I.; Lee, C.; Wang, L.; Sorgenfrei, S.; Watanabe, K.; Taniguchi, T.; Kim, P.; Shepard, K. L.; Hone, J. *Nat. Nanotechnol.* **2010**, *5*, 722−726.
(2) Britnell, L.; Gorbachev, R. V.; Jalil, R.; Belle, B. D.; Schedin, F.; Mishchenko, A.; Georgiou, T.; Katsnelson, M. I.; Eaves, L.; Morozov, S. V.; Peres, N. M. R.; Leist, J.; Geim, A. K.; Novoselov, K. S.; Ponomarenko, L. A. *Science* **2012**, *335*, 947−950.
(3) Geim, A. K.; Grigorieva, I. V. *Nature* **2013**, *499*, 419−425.
(4) Geim, A. K. *Science* **2009**, *324*, 1530−1534.
(5) Castro Neto, A. H.; Guinea, F.; Peres, N. M. R.; Novoselov, K. S.; Geim, A. K. *Rev. Mod. Phys.* **2009**, *81*, 109−162.
(6) Zhang, Y. B.; Tan, Y. W.; Stormer, H. L.; Kim, P. *Nature* **2005**, *438*, 201−204.
(7) Wang, L.; Chen, Z.; Dean, C. R.; Taniguchi, T.; Watanabe, K.; Brus, L. E.; Hone, J. *ACS Nano* **2012**, *6*, 9314−9319.
(8) Balakrishnan, J.; Koon, G. K. W.; Jaiswal, M.; Neto, A. H. C.; Oezyilmaz, B. *Nat. Phys. Lett.* **2013**, *9*, 284−287.
(9) Ryu, S.; Han, M. Y.; Maultzsch, J.; Heinz, T. F.; Kim, P.; Steigerwald, M. L.; Brus, L. E. *Nano Lett.* **2008**, *8*, 4597−4602.
(10) Kim, K. S.; Zhao, Y.; Jang, H.; Lee, S. Y.; Kim, J. M.; Kim, K. S.; Ahn, J.-H.; Kim, P.; Choi, J.-Y.; Hong, B. H. *Nature* **2009**, *457*, 706−710.
(11) Huh, S.; Park, J.; Kim, Y. S.; Kim, K. S.; Hong, B. H.; Nam, J. M. *ACS Nano* **2011**, *5*, 9799−9806.

dx.doi.org/10.1021/nl5036012 | *Nano Lett.* XXXX, XXX, XXX−XXX

(12) Cancado, L. G.; Jorio, A.; Martins Ferreira, E. H.; Stavale, F.; Achete, C. A.; Capaz, R. B.; Moutinho, M. V. O.; Lombardo, A.; Kulmala, T. S.; Ferrari, A. C. *Nano Lett.* **2011**, *11*, 3190−3196.
(13) Lucchese, M. M.; Stavale, F.; Ferriera, E. H.; Vilane, C.; Moutinho, M. V. O.; Capaz, R. B.; Achete, C. A.; Jorio, A. *Carbon* **2010**, *48*, 1592−1597.
(14) Eckmann, A.; Felten, A.; Verzhibitskiy, I.; Davey, R.; Casiraghi, C. *Phys. Rev. B* **2013**, *88*, 035426.
(15) Goler, S.; Coletti, C.; Tozzini, V.; Piazza, V.; Mashoff, T.; Beltram, F.; Pellegrini, V.; Heun, S. *J. Phys. Chem. C* **2013**, *117*, 11506−11513.
(16) Tozzini, V.; Pellegrini, V. *J. Phys. Chem. C* **2011**, *115*, 25523−25528.
(17) Wang, Q. H.; Jin, Z.; Kim, K. K.; Hilmer, A. J.; Paulus, G. L. C.; Shih, C.-J.; Ham, M.-H.; Sanchez-Yamagishi, J. D.; Watanabe, K.; Taniguchi, T. *Nat. Chem.* **2012**, *4*, 724−732.
(18) Yamamoto, M.; Einstein, T. L.; Fuhrer, M. S.; Cullen, W. G. *ACS Nano* **2012**, *6*, 8335−8341.
(19) Adam, S.; Jung, S.; Klimov, N. N.; Zhitenev, N. B.; Stroscio, J. A.; Stiles, M. D. *Phys. Rev. B* **2011**, *84*, 235421.
(20) Georgakilas, V.; Otyepka, M.; Bourlinos, A. B.; Chandra, V.; Kim, N.; Kemp, K. C.; Hobza, P.; Zboril, R.; Kim, K. S. *Chem. Rev.* **2012**, *112*, 6156−6214.
(21) Johns, J. E.; Hersam, M. C. *Acc. Chem. Res.* **2013**, *46*, 77−86.
(22) Jung, J.; García-González, P.; Dobson, J. F.; Godby, R. W. *Phys. Rev. B* **2004**, *70*, 205107.
(23) Marini, A.; Garcia-Gonzalez, P.; Rubio, A. *Phys. Rev. Lett.* **2006**, *96*, 136404.
(24) Lebegue, S.; Harl, J.; Gould, T.; Angyan, J. G.; Kresse, G.; Dobson, J. F. *Phys. Rev. Lett.* **2010**, *105*, 196401.
(25) Bjorkman, T.; Gulans, A.; Krasheninnikov, A. V.; Nieminen, R. M. *Phys. Rev. Lett.* **2012**, *108*, 235502.
(26) Tozzini, V.; Pellegrini, V. *Phys. Chem. Chem. Phys.* **2013**, *15*, 80−89.
(27) Ströbel, R.; Garche, J.; Moseley, P. T.; Jörissen, L.; Wolf, G. *J. Power Sources* **2006**, *159*, 781−801.

dx.doi.org/10.1021/nl5036012 | *Nano Lett.* XXXX, XXX, XXX−XXX